Semiclassical Treatment of Thermally Activated Electron Transfer in the Intermediate to Strong Electronic Coupling Regime under the Fast Dielectric Relaxation.

ARTICLE *in* THE JOURNAL OF PHYSICAL CHEMISTRY A · JANUARY 2009

Impact Factor: 2.69 · DOI: 10.1021/jp810914v · Source: PubMed

3 AUTHORS:

Yi Zhao
Xiamen University
89 PUBLICATIONS **1,165** CITATIONS
SEE PROFILE

WanZhen Liang
Xiamen University
76 PUBLICATIONS **2,525** CITATIONS
SEE PROFILE

Hiroki Nakamura
National Chiao Tung University
238 PUBLICATIONS **4,089** CITATIONS
SEE PROFILE

Semiclassical Treatment of Thermally Activated Electron Transfer in the Intermediate to Strong Electronic Coupling Regime under the Fast Dielectric Relaxation

Yi Zhao,*,† Wanzhen Liang,† and Hiroki Nakamura‡

Hefei National Laboratory for Physical Sciences at Microscale and Department of Chemical Physics, University of Science and Technology of China, Hefei, 230026, P. R. China, and Department of Theoretical Studies, Institute for Molecular Science, National Institutes of Natural Sciences, Myodaiji, Okazaki 444-8585, Japan

Received: March 12, 2006; In Final Form: May 11, 2006

The generalized nonadiabatic transition-state theory (NA-TST) (Zhao, Y.; et al. *J. Chem. Phys.* **2004**, *121*, 8854) is used to study electron transfer with use of the Zhu−Nakamura (ZN) formulas of nonadiabatic transition in the case of fast dielectric relaxation. The rate constant is expressed as a product of the well-known Marcus formula and a coefficient which represents the correction due to the strong electronic coupling. In the case of general multidimensional systems, the Monte Carlo approach is utilized to evaluate the rate by taking into account the multidimensionality of the crossing seam surface. Numerical demonstration is made by using a model system of a collection of harmonic oscillators in the Marcus normal region. The results are naturally coincident with the perturbation theory in the weak electronic coupling limit; while in the intermediate to strong electronic coupling regime where the perturbation theory breaks down the present results are in good agreement with those from the quantum mechanical flux−flux correlation function within the model of effective one-dimensional mode.

1. Introduction

The present paper is an extension of our earlier work[1] for the discussion of nonadiabatic chemical reactions to electron transfer (ET) in the intermediate to strong electronic coupling in the limit of fast solvent relaxation. In the previous paper, we incorporated the Zhu−Nakamura (ZN) theory for the two-state curve crossing problem into the nonadiabatic transition-state theory (NA-TST). The approach has been applied to the one- and two-dimensional systems with exponential and Morse diabatic potential energy surfaces (PES) and exponential diabatic coupling. The numerical results demonstrated its potential applicability.

The ET in the strong electronic coupling regime is frequently related to the solvent dynamical relaxation processes. In this case, the electronic coupling itself may not be a sufficient factor to justify the usage of nonadiabatic or adiabatic theory. If the solvent relaxation is very slow compared with the ET process, then multiple crossings of the transition region become possible even in the weak coupling region. As a result, higher order perturbation with respect to the electronic coupling is required. Ultimately, the reactions can become independent of the electronic coupling, that is, they become solvent-controlled adiabatic reactions while still nonadiabatic in the absence of solvent dynamics. On the basis of the original works independently done by Zusman[2] and Burshtein and co-workers,[3] a large number of theoretical approaches have been proposed to treat the competition between solvent relaxation and electronic transitions in the case of strong coupling (see, for instance, ref 4 and references therein). Yet, the true adiabatic process is different from the nonadiabatic one with slow solvent polarization modes. Several works have clarified the differences.[5−7] In the limit of fast dielectric relaxation, on the other hand, ET rate is independent of the relaxation properties of the solvent and the traditional thermal equilibrium formulation is applicable. In the present paper, we will study the ET in this limit, while leaving the discussions on the solvent dynamical effects for future study.

From the very beginning of the development of the ET theory,[8−11] it has been recognized that the perturbation theory is applicable for a weak coupling regime (nonadiabatic limit) and the adiabatic transition-state theory can be used in the strong coupling limit to describe reactions as taking place on the adiabatic PES. Since then, numerous attempts have been undertaken to try to develop a unified theory to incorporate these two limits in a consistent way.[12−20]

The classical and semiclassical treatments of ET thermal rate have a long history, and the well-known Marcus−Hush semiclassical formula[9,21] has been continuously used in the field. In this formula, the thermally averaged Landau−Zener (LZ) transmission probability[22−24] is used to connect the nonadiabatic and adiabatic limits. The nuclear tunneling effect is additionally incorporated independently from the electronic transition, which cannot be a proper procedure since the electronic transition and nuclear tunneling cannot be separated.

To treat multidimensional ET problems, the idea of effective frequency is introduced to match the multi-mode LZ transmission coefficient.[25,26] The validity of the one-dimensional model based on the LZ formula, however, is criticized (see, e.g., ref 4) when it is applied to a system of reaction coordinates coupled to a bath. Rips and Pollak[27,28] have introduced an optimized reaction coordinate to solve this problem. They use a canonical transformation to optimize the reaction path and maximize its mean free path in the vicinity of the crossing point. When the

* To whom correspondence should be addressed. E-mail: yizhao@ustc.edu.cn.
† University of Science and Technology of China.
‡ National Institutes of Natural Sciences.

10.1021/jp061513g CCC: $33.50
Published on Web 06/10/2006

mean free path is longer than the characteristic LZ length, the LZ formula is applicable.

The electron transfer in a multidimensional space can be directly treated by using the surface hopping technique[29−33] without explicitly introducing a one-dimensional reaction coordinate in configuration space. The transition probability is evaluated on the seam surface in the instantaneous normal-mode coordinates of the system by taking the momentum along the direction of the mode normal to the seam surface. On the basis of the surface hopping approach, a variety of NA-TSTs have been developed in the study of nonadiabatic chemical reactions. Zahr, Preston, and Miller[34] established a phase space integral formulation in the diabatic representation where the locus of intersection of potential energy surfaces (PES) plays the role of the seam surface. Heller and Brown[35] have also utilized the rate formula in the scope of the phase space integral. Lorquet and Leyh-Nihant[36,37] developed the statistical Rice−Ramsperger−Kassel−Marcus (RRKM)-like equation for nonadiabatic unimolecular reactions. Marks and Thompson[38,39] introduced a weighted flux through the seam surface and obtained the nonadiabatic transition-state formula in the phase space. Topaler and Truhlar[40] studied the nonadiabatic decay rate of the excited complex in the scope of the statistical model. Using the minimum energy crossing point (MECP) as the hopping point, Cui[41] developed a theory which is very similar to the original adiabatic transition-state theory by Miller.[42] In most of these NA-TSTs, the nonadiabatic transition probability is given by the LZ formula. It is well-known, however, that the LZ theory does not work at energies near or lower than the crossing point, that is, it cannot incorporate the classically forbidden nonadiabatic transitions. Besides, the LZ probability is not very accurate for the case of strong diabatic coupling. Furthermore, the LZ theory requires information from diabatic PESs, which is not available in general.

In the present work, we utilize the generalized NA-TST[1] and the ZN theory to formulate a new formula similar to the Marcus formula. The purpose is to propose a simple yet accurate formula to be directly applicable to explain experimental data, for example, the localized-to-delocalized ET in mixed-valence molecules.[43,44] The formulation can also be used to define the "sink" function[45−47] along the fast vibrational modes in the treatment of solvent-controlled ET reactions. The difference from the Marcus formula is the prefactor which is defined by the thermally averaged ZN formula. The generalized NA-TST is formulated based on Miller's reactive flux−flux correlation function approach. The Zhu−Nakamura (ZN) theory,[48−52] on the other hand, is practically free from the drawbacks of the LZ theory mentioned above. It covers all of the energy range in the two-state curve crossing problem and can be implemented in practice using only the adiabatic PESs information. Numerical tests[1] have also shown that it is very essential for accurate evaluation of the thermal rate constant to take into account the multidimensional topography of the seam surface and treat the nonadiabatic electronic transition and nuclear tunneling effects properly. The presently proposed formula of ET rate is applicable to multidimensional systems and the Monte Carlo approach can be usefully utilized. The numerical tests for a multidimensional harmonic system in the Marcus normal region demonstrate that the present formula can cover a wide temperature range from deep tunneling to classical high temperature. In the weak coupling regime, it gives excellent agreement with the Bixon−Jortner[53] formula. In the strong electronic coupling regime, rigorous quantum mechanical evaluation of the ET rate is nontrivial for multidimensional systems even in the limit of fast relaxation. The numerical tests of the present approach have found that the matching technique to fit multi-mode by one effective mode[25] can give a very good result in the wide range of electronic coupling strength and temperature except in the deep tunneling region for symmetric ET reactions. Thus, instead of carrying out computations of a multidimensional system directly, we can rigorously evaluate the ET rate by the quantum mechanical flux−flux correlation function method[54] within the effective one-dimensional model in both the nonadiabatic and adiabatic regimes. The present semiclassical results are found to be in good agreement with the quantum ones in the whole range of coupling strength.

Since the ZN formulas are applicable to both harmonic and anharmonic PESs with coordinate-dependent electronic coupling, the present approach can directly treat general cases of anharmonic potentials with the non-Condon effect taken into account.

This paper is organized as follows. In section 2, we summarize the formulation of NA-TST. Section 3 derives a new formula which modifies the Marcus formula starting from this NA-TST. The Monte Carlo implementation for multidimensional systems is shown in section 4. Section 5 presents numerical applications to the multidimensional collective oscillator model for both symmetric and asymmetric reactions. Section 6 is the conclusion. Appendices A and B present the ZN formulas used in the nonadiabatic tunneling case and the explanation of the effective one-dimensional model.

2. Generalized Nonadiabatic Transition-State Theory

The rigorous quantum mechanical ET rate constant is written by the flux-side correlation function[54] as

$$kZ_r = \lim_{t\to\infty} \mathrm{tr}[\mathrm{e}^{-\beta\hat{H}}\,\hat{F}\mathrm{e}^{i\hat{H}t/\hbar}\hat{h}\mathrm{e}^{-i\hat{H}t/\hbar}] \tag{1}$$

Here Z_r is the partition function of the donor, $\hat{H}$ is the Hamiltonian of the system, $\hat{h}$ is Heaviside function, $\hat{F} = i/\hbar[\hat{H}, \hat{h}]$ is the flux operator through the dividing surface between reactants and products, and $\beta = 1/\kappa T$ as usual. Within the framework of the transition-state theory, eq 1 is cast into[1]

$$k = Z_{\mathrm{mod}}Z_{\mathrm{cl}}^{-1}\sqrt{\frac{1}{2\pi\beta}} \int \mathrm{d}\mathbf{Q}\ \mathrm{e}^{-\beta V_1(\mathbf{Q})}\,P_T(\beta,\mathbf{Q})\,|\nabla S(\mathbf{Q})|\delta(\xi_0 - S(\mathbf{Q})) \tag{2}$$

for an N-dimensional system. Here, $Z_{\mathrm{cl}} = \int \mathrm{d}\mathbf{Q}\ \mathrm{e}^{-\beta V_1(\mathbf{Q})}$ is the classical partition function of the donor and Z_{mod} is the quantum mechanical correction of the partition function, and its definition is explicitly given in ref 1, $\mathbf{Q}$ represents the nuclear Cartesian coordinates of N degrees of freedom, $V_1(\mathbf{Q})$ is the potential energy surface of the donor, and $\xi = \xi_0 = S(\mathbf{Q})$ determines the crossing seam surface from the donor to the acceptor. The variable ξ is introduced to define the free energy (see the next section). The effective transition probability $P_T(\beta,\mathbf{Q})$ at a given temperature T is evaluated from the nonadiabatic transition probability $P_{\mathrm{ZN}}(E,\mathbf{Q})$ by

$$\mathrm{P}_T(\beta,\mathbf{Q}) = \beta\int_0^\infty \mathrm{d}E\ \mathrm{e}^{-\beta(E-V_1(\mathbf{Q}))}\,P_{\mathrm{ZN}}(E,\mathbf{Q}) \tag{3}$$

where E represents the total energy along the direction normal to the seam surface at the nuclear coordinates $\mathbf{Q}$. We implement $P_{\mathrm{ZN}}(E,\mathbf{Q})$ by the ZN formulas[50−52] which can cover the whole energy range from the deep tunneling to high-energy regions with high accuracy. The details of the ZN formulas are given

in Appendix A. The basic physical idea behind eq 2 is the surface hopping due to nonadiabatic transition[29−31] which has been widely used in the study of nonadiabatic chemical reactions.

3. Improvement of the Marcus Formula

In the original Marcus formula, the rate is described by using the free energy. To find the connection between eq 2 and the Marcus formula, we introduce the free energy profile $F_1(\xi)$ by

$$e^{-\beta F_1(\xi)} = \int d\mathbf{Q}\, e^{-\beta V_1(\mathbf{Q})} |\nabla S(\mathbf{Q})|\, \delta(\xi - S(\mathbf{Q})) \quad (4)$$

Equation 2 can then be recast into

$$k = Z_{mod} Z_{cl}^{-1} \sqrt{\frac{1}{2\pi\beta}}\, \bar{P}_T(\beta,\xi_0) \int d\xi \delta(\xi - \xi_0) e^{-\beta F_1(\xi)} \quad (5)$$

where the average transition probability $\bar{P}_T(\beta,\xi)$ is defined by

$$\bar{P}_T(\beta,\xi) = \frac{\int d\mathbf{Q}\, e^{-\beta V_1(\mathbf{Q})} |\nabla S(\mathbf{Q})|\, \delta(\xi - S(\mathbf{Q})) P_T(\beta,\mathbf{Q})}{\int d\mathbf{Q}\, e^{-\beta V_1(\mathbf{Q})} |\nabla S(\mathbf{Q})|\, \delta(\xi - S(\mathbf{Q}))} \quad (6)$$

In the linear response limit, the free energies $F_i(\xi)$ ($i = 1, 2$) of the donor and acceptor can be expressed by parabolic functions of ξ as

$$F_1(\xi) = -\frac{1}{\beta} \ln[\int d\mathbf{Q}\, e^{-\beta V_1(\mathbf{Q})} |\nabla S(\mathbf{Q})|\, \delta(\xi - S(\mathbf{Q}))] = \frac{1}{2}\omega^2(\xi - \xi_{01})^2 \quad (7)$$

and

$$F_2(\xi) = -\frac{1}{\beta} \ln[\int d\mathbf{Q}\, e^{-\beta V_2(\mathbf{Q})} |\nabla S(\mathbf{Q})|\, \delta(\xi - S(\mathbf{Q}))] = \frac{1}{2}\omega^2(\xi - \xi_{02})^2 + \Delta G \quad (8)$$

where ξ_{01} and ξ_{02} are the positions of the donor and acceptor free energy minima, respectively, and ΔG represents the exothermicity of the reaction which is determined by setting $\xi = \xi_{02}$ in eq 8.

By the use of the free energy definition of eq 7, the partition function Z_{cl} can be cast to

$$Z_{cl} = \int d\xi\, e^{-\beta V_1(\xi)} \quad (9)$$

Combining eqs 5, 7, and 9, we can obtain

$$k = \kappa k_{Marcus} \quad (10)$$

with

$$\kappa = \frac{\hbar\omega}{2\pi H_{AB}^2} \sqrt{\frac{\lambda}{\pi\beta}}\, \bar{P}_T(\beta,\xi_0) \quad (11)$$

where k_{Marcus} is the Marcus formula given by

$$k_{Marcus} = \frac{H_{AB}^2}{\hbar} \sqrt{\frac{\pi\beta}{\lambda}}\, e^{-\beta(\lambda+\Delta G)^2/4\lambda} \quad (12)$$

and H_{AB} is the electronic coupling between donor and acceptor. The reorganization energy λ is defined by

$$\lambda = \frac{1}{2}\omega^2(\delta\xi_0)^2 \quad (13)$$

where $\delta\xi_0 = \xi_{02} - \xi_{01}$. In eq 10, the effects of nonadiabatic transition and tunneling are properly taken into account by κ and naturally the main task is to evaluate the average transition probability $\bar{P}_T(\beta,\xi)$.

Let us consider the nonadiabatic reaction along the one-dimensional coordinate ξ. The free energy curves act as potential curves, and eq 6 becomes

$$\bar{P}_T(\beta,\xi_0) = \beta \int_0^\infty dE\, e^{-\beta E} P_{ZN}(E,\xi_0) \quad (14)$$

where $P_{ZN}(E,\xi_0)$ is determined from the free energy profiles. At high temperatures and a weak electronic coupling limit, $P_{ZN}(E,\xi_0)$ can be given by the Taylor expansion of the LZ or ZN formula as

$$P_{ZN}(E,\xi_0) = \frac{2\pi H_{AB}^2}{\hbar|\Delta F|\sqrt{2E}} \quad (15)$$

where ΔF is the slope difference of the two diabatic potentials at the crossing point. Combining eqs 15, 14, and 11, one can easily find $\kappa = 1$. Thus, eq 10 goes back to the original Marcus formula in the nonadiabatic (weak electronic coupling) limit. When the coupling strength becomes strong enough, eq 10 reads

$$k = \frac{\omega}{2\pi} e^{-\beta(\lambda+\Delta G)^2/4\lambda} \quad (16)$$

under the condition $P_{ZN}(E,\xi_0) = 1.0$. Equation 16 is nothing but the Marcus formula in the adiabatic limit.

4. Monte Carlo Implementation of Multidimensional Case

In the previous section, we have clarified the relation between eq 5 and the Marcus theory eq 12. In this section, we mainly focus on the numerical implementation for multidimensional systems.

To use the Monte Carlo technique, it is natural to rewrite eq 5 as a product of two contributions, namely

$$k = Z_{mod} \sqrt{\frac{1}{2\pi\beta}}\, R_1 R_2 \quad (17)$$

with

$$R_1 = \frac{\int d\mathbf{Q}\, e^{-\beta V_1(\mathbf{Q})} |\nabla S(\mathbf{Q})|\, \delta(\xi_0 - S(\mathbf{Q}))}{\int d\xi \int d\mathbf{Q}\, e^{-\beta V_1(\mathbf{Q})} |\nabla S(\mathbf{Q})|\, \delta(\xi - S(\mathbf{Q}))} \equiv \frac{F_1(\xi_0)}{Z_{cl}} \quad (18)$$

and

$$R_2 = \frac{\int d\mathbf{Q}\, e^{-\beta V_1(\mathbf{Q})} |\nabla S(\mathbf{Q})|\, \delta(\xi_0 - S(\mathbf{Q})) P_T(\beta,\mathbf{Q})}{\int d\mathbf{Q}\, e^{-\beta V_1(\mathbf{Q})} |\nabla S(\mathbf{Q})|\, \delta(\xi_0 - S(\mathbf{Q}))} \equiv \bar{P}_T(\beta,\xi_0) \quad (19)$$

Here, R_1 represents the ratio of the free energy on the seam surface and the reactant partition function Z_{cl}, and R_2 corresponds to the average nonadiabatic transition probability at the seam surface $S(\mathbf{Q}) - \xi_0 = 0$.

The seam surface is defined as the crossing of the donor and acceptor potentials, that is, defined by the equation $\xi = \xi_0 =$

$V_1 - V_2 = 0$, which corresponds to $S(\mathbf{Q}) = V_1(\boldsymbol{Q}) - V_2(\boldsymbol{Q})$ and $\xi_0 = 0$. To evaluate the δ function of the seam surface in eqs 18 and 19, the molecular dynamics (MD) method may be convenient in combination with the SHAKE algorithm.[55] On the other hand, in the MC approach, one may replace the δ function by a Gaussian function with sufficiently small width. In this work, we employ an alternative approach, that is, the simplified adaptive umbrella sampling approach[56,57] along the reaction coordinate ξ combined together with the histogram technique, in which the δ function in the sampling is defined automatically if the histogram width is small enough.

It is noted that $F_1(\xi_0)$ is a property associated with the potential at the transition state, while Z_{cl} is associated with the bottom of the donor well. The direct MC approach fails in most cases of the evaluation of this ratio especially at low temperatures, because the system will seldom visit the transition state due to the exponentially small probability density there. This is a well-known problem associated with statistical sampling of rare events. In such a case, the umbrella sampling technique is commonly used, in which an artificial potential is added to the system to bias the sampling toward the transition state to overcome very poor statistics resulting from the conventional MC method.

To achieve this, we divide a large enough interval of the reaction coordinate ξ, which should cover all the contribution to the partition function Z_{cl}, into n equal slices, that is, bins. In each bin, we add a biasing potential $U(\xi_i)$. Then, the biased probability becomes

$$P(\xi_i) = f(\xi_i)P_0(\xi_i) \tag{20}$$

where the unbiased probability is given by

$$P_0(\xi_i) = \int \mathrm{d}\mathbf{Q}\, \mathrm{e}^{-\beta V_1(\mathbf{Q})} |\nabla S(\mathbf{Q})|\, \delta(\xi_i - S(\mathbf{Q})) \tag{21}$$

and the coefficient $f(\xi_i)$ is defined as

$$f(\xi_i) = \exp(-\beta U(\xi_i)) \tag{22}$$

The biasing potential $U(\xi_i)$ is chosen so that the biased probability $P(\xi_i)$ is as flat as possible. In the MC simulation, one may choose the weighted function as $\exp[-\beta(V_1(\mathbf{Q}) + U(\xi_i))]$. Thus, R_1 can be obtained by

$$R_1 = \frac{P(\xi_0)(f(\xi_0))^{-1}}{\int \mathrm{d}\xi\, P(\xi)(f(\xi))^{-1}} \tag{23}$$

However, we do not know $U(\xi_i)$ a priori. An iterative learning procedure has to be employed to determine it, such as the weighted histogram analysis method (WHAM).[55] Recently, Wang and Landau[58] introduced an effective MC approach to evaluate the density of states for complex systems. Here, we use a similar trick to modify the coefficient $f(\xi_i)$ in each iteration with the replacement of $f(\xi_i)$ by $f(\xi_i)/P(\xi_i)$ and then proceed to the next iteration with this new $f(\xi_i)$ until the $P(\xi_i)$ becomes uniform (see more detail in refs 56 and 57). It should be mentioned that the width in the WHAM is small enough for each bin to represent $\delta(\xi)$.

Although the evaluation of R_2 can be achieved, in principle, by the conventional MC technique, the same method as in the calculation of R_1 would be more efficient. We choose a small range of ξ around ξ_0 and let the MC random walk visit this range. At $\xi = \xi_0$, we evaluate the nonadiabatic transition probability eq 3 numerically. In this way, the MC walk is easier to sample the whole important range on the seam surface than the conventional way.

TABLE 1: Frequencies and Reorganization Energies of the 12-Dimensional Harmonic Oscillator Model

ω_i (cm^{-1})	λ_i (cm^{-1})	ω_i (cm^{-1})	λ_i (cm^{-1})
462	3038	1007	269
511	1372	1169	638
584	775	1252	351
602	1039	1334	625
628	2125	1403	275
677	1196	1548	100

5. Numerical Examples

5.1. Collective Harmonic Oscillator Model. Despite the fact that the formula is applicable to general systems, for the purpose of comparison with the perturbation theory, we consider a model system often used in the study of ET in which the donor and the acceptor are considered as a collection of shifted harmonic oscillators. The Hamiltonians are thus expressed as

$$H_1 = \sum_i \frac{P_i^2}{2} + V_1 \tag{24}$$

and

$$H_2 = \sum_i \frac{P_i^2}{2} + V_2 \tag{25}$$

with the potential energy surfaces

$$V_1 = \frac{1}{2}\sum_i \omega^2{}_i Q_i^2 \tag{26}$$

and

$$V_2 = \frac{1}{2}\sum_i \omega^2{}_i (Q_i - Q_{0i})^2 \tag{27}$$

where H_1 and H_2 correspond to the donor and acceptor, respectively. The parameter ω_i and reorganization energy $\lambda_i = 1/2(\omega_i^2 Q_{0j}^2)$ are listed in Table 1. In all the simulations, the exothermicity ΔG of the reaction is set to zero. The reaction coordinate ξ thus is defined as

$$\xi = V_1 - V_2 = \sum_j \left(\omega_j{}^2 Q_j - \frac{1}{2}\omega^2 Q_{0j}{}^2\right) \tag{28}$$

while the seam surface corresponds to $\xi = \xi_0 = 0$.

Figure 1 shows the free energy curves with respect to ξ for the donor and the acceptor. The ground adiabatic state is denoted by asterisks. In the simulation, 1×10^8 points are taken in the MC circle. In the collection of harmonic oscillators, the free energy profiles have the analytical forms as

$$F_1(\xi) = \frac{1}{4\lambda}(\xi + \lambda)^2 \tag{29}$$

and

$$F_2(\xi) = \frac{1}{4\lambda}(\xi - \lambda)^2 \tag{30}$$

where the zero energy at $\xi = \lambda$ is taken as reference and the total reorganization energy λ is given by $\lambda = \sum_i \lambda_i$. Our numerical

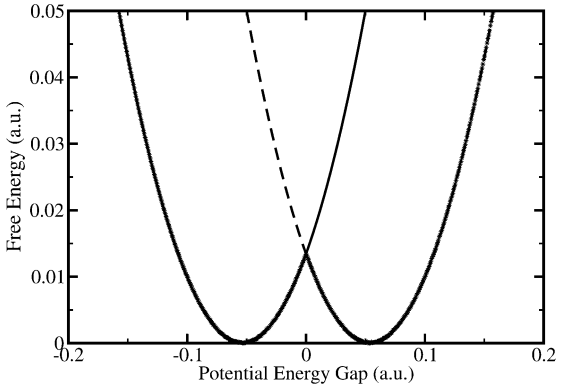

Figure 1. Free energy profiles corresponding to the potentials defined in section 5.1 (see also Table 1). The electronic coupling strength used is $H_{AB} = 0.0001$ au. The solid line is for the donor, the dashed line for the acceptor, and the asterisk is the ground-state free energy in the adiabatic representation.

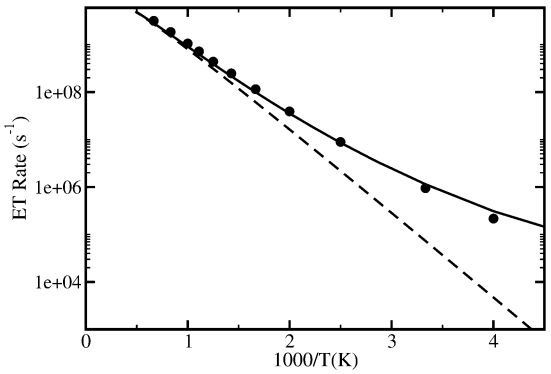

Figure 2. Arrhenius plot of the ET rate. The electronic coupling strength is $H_{AB} = 0.0001$ au. The solid line represents the Bixon−Jortner perturbation theory;[59] the full circle represents the present result (eq 10); the dashed line represents Marcus's high-temperature theory (eq 12).

values are in excellent agreement with those from eqs 29 and 30, which demonstrates the accuracy of the present MC technique (the analytical values are not shown in Figure 1 because of indistinguishability).

The evaluation of R_2, namely, $\bar{P}_T(\beta,\xi_0)$, is the most CPU time-consuming. To get a fast convergence of R_2 and save computer time, we calculate $\bar{P}_T(\beta,\xi_0)$ once every 10 MC visits of the seam surface. The convergence is achieved within 1×10^4 evaluations of $\bar{P}_T(\beta,\xi_0)$.

In Figure 2a, we show the ET rate against temperature in the weak electronic coupling regime (nonadiabatic limit). In the evaluation, the partition function correction is obtained via normal-mode analysis in the reactive well and MECP. For a comparison, the rate evaluated from the Bixon−Jortner (BJ) approach (eq 3.9 in ref 59) is also shown by the solid line. The present results are in very good agreement with those from the BJ formula in the whole temperature range except in the deep tunneling regime where the error at temperature $T = 250$ K is only 29%. This figure also shows the results from the Marcus formula eq 12. As expected, the results from the Marcus formula become too small as the temperature decreases because of neglecting nuclear tunneling effect. The slope of the rate with respect to temperature in the case of Marcus formula is mainly determined by the transition-state barrier height.

The fact that the electronic transition and nuclear tunneling cannot be separated can be clearly seen from the ZN theory.[48−52] Significance of the nonadiabatic tunneling effect at low temperatures is clearly demonstrated in Figure 3, where R_2 based

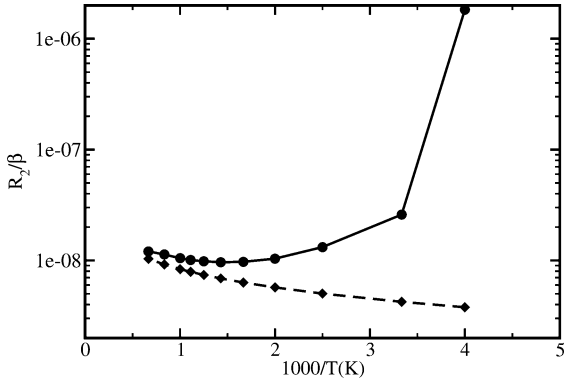

Figure 3. Effect of nonadiabatic tunneling. The solid line with circle is R_2/β with use of the ZN formula, and the dashed line with diamond is R_2/β with use of the LZ formula. The parameters used are the same as those in Figure 2.

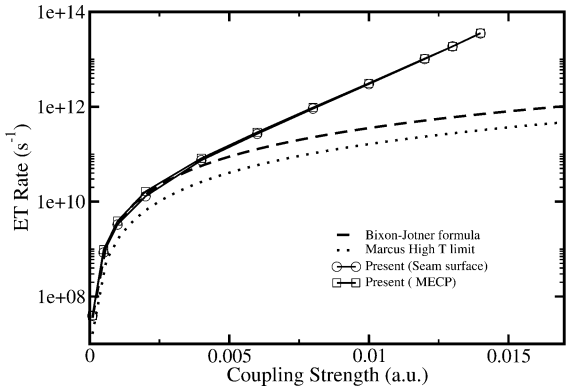

Figure 4. ET rate vs electronic coupling strength H_{AB}. The temperature is $T = 500$ K. The solid line with circle shows the present result (eq 10) with the transition probability averaged over the seam surface; the solid line with square shows the present result (eq 10) with the transition probability taken at the minimum energy crossing point (MECP); the dashed line shows the result of the Bixon−Jortner theory;[59] the dotted line shows the result of Marcus's high-temperature theory (eq 12).

on the ZN formulas is compared with that of the LZ formula. One can roughly say that the pure electronic transition dominates at $T > 900$ K and the joint effect of electronic transition and nuclear tunneling becomes crucial at $T < 400$ K. This is consistent with the result of Figure 2 where the Marcus theory works well only at $T > 900$ K.

Figure 4 shows the ET rate against the electronic coupling strength H_{AB} at $T = 500$ K. In the evaluation of the present formula, eq 10, two different values of $\bar{P}_T(\beta,\xi)$ are considered: one is the direct evaluation of eq 19, namely, the transition probability is averaged over the seam surface (generalized transition-state theory) and the other is to simply take a constant value at the minimum energy crossing point (MECP) as in the conventional transition-state theory. In the latter case, the seam surface $S(\mathbf{Q})$ is implicitly replaced by $S(\mathbf{Q}_0)$ in the evaluation of the transition probability $\bar{P}_T(\beta,\xi)$, where $\mathbf{Q}_0$ is the position of the MECP. The difference between the two methods is only 10%, and the second method might be considered to be good enough. It should be noted, however, that this is simply because the electronic coupling is constant and the potentials are simple in the present model. The MECP method can easily produce very poor results especially when the electronic coupling depends on the coordinates.[1] In Figure 4, we also show the rates from the BJ and Marcus theories. It is easily seen that, while the results of our formula and the BJ approach are consistent in the nonadiabatic limit ($H_{AB} < 0.0025$ au), the latter naturally breaks down as the coupling increases. In the strong coupling

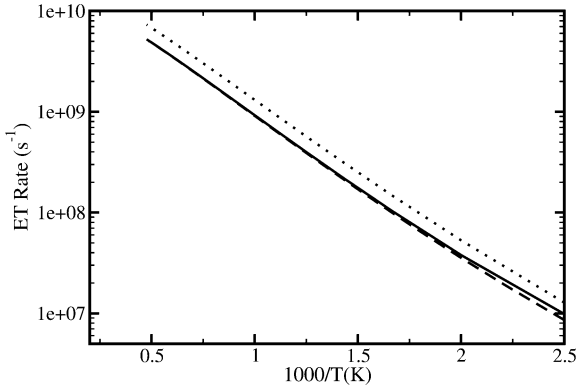

Figure 5. Arrhenius plot of the ET rate in the effective one-dimensional model. The electronic coupling strength is $H_{AB} = 0.0001$ au. The solid line represents the present full-dimensional result; the dashed line represents the one-dimensional model with $\omega_2 = 749$ cm^{-1}; the dotted line represents the one-dimensional model with $\omega_1 = 1027$ cm^{-1}.

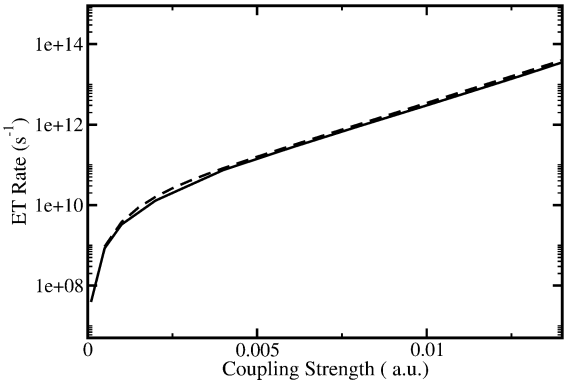

Figure 6. ET rate vs the electronic coupling strength H_{AB} at $T = 500$ K. The solid line shows the present full-dimensional result; the dashed line shows the present result in the effective one-dimensional model; the filled circle shows the result of the quantum mechanical flux−flux correlation function; the dotted line shows the quantum mechanical result in the adiabatic approximation. In the case of effective one-dimensional model, the effective frequency is taken as $\omega_2 = 749$ cm^{-1}.

regime, the Marcus−Hush formula[9,21] is often used to explain experimental data. In the one-dimensional model, however, we have found that the Marcus−Hush formula based on the LZ formula gives poor results at low temperatures. On the other hand, eq 10 reproduces the quantum rate excellently in wide ranges of coupling and temperature.

5.2. Effective One-Dimensional Model. It would be very useful and convenient for the interpretation of experimental data, if we can match the collection of harmonic oscillators to a certain effective one-dimensional harmonic model. This matching technique is especially useful, if the frequencies and reorganization energies of individual modes are not available. Dogonadze[25] has proposed the effective one-dimensional frequency (see eq B-6 in Appendix B) by fitting the prefactor in the multidimensional system under the LZ approximation to that in the effective one-dimensional system. For the purpose of comparison, here we consider two kinds of matching techniques. Since the nonadiabatic transition probability is determined along the direction normal to the seam surface, one may take the effective one-dimensional model along that direction with the effective frequency ω_1 (see eq B-3 in Appendix B). The one-dimensional potentials are given by eqs B-1 and B-2. The second method, on the other hand, is to use the effective frequency ω_2 (see eq B-6 in Appendix B) defined by Dogonadze.

In the case of the above-mentioned effective one-dimension model, eq 17 can be rewritten as

$$k = \frac{2}{h\beta}\sinh\left(\frac{\hbar\omega\beta}{2}\right)\int_0^\infty \mathrm{d}E\,\exp(-\beta E)P_{ZN}(E) \qquad (31)$$

In Figure 5, we show the ET rate as a function of temperature in the weak coupling case ($H_{AB} = 0.0001$ au). The two effective frequencies used are $\omega_1 = 1027$ cm^{-1} and $\omega_2 = 749$ cm^{-1}, respectively. Comparing with the result from the multidimensional calculation, we can see that the rate is too large in the case of ω_1, while the rate with ω_2 (Dogonadze frequency) is in excellent agreement with that of the multidimensional simulation except in the deep tunneling regime. In the first method of using ω_1, the nonadiabatic probability is taken at the MECP which gives the maximum value in the present model and the reactant partition function predicted is too small compared with the multidimensional one. Both effects give large contributions to the rate. This indicates that, despite that one may use the MECP as the transition state, the one-dimensional model along the MECP cannot produce good results.

In Figure 6, the ET rate by the second method of using the effective frequency ω_2 is compared with the multidimensional simulation in a wide range of coupling strength. Again, this one-dimensional model works nicely. We can conclude that the effective model in which the effective frequency is defined by the method of Dogonadze can be a very good approximation at least for a collection of harmonic oscillators with the Condon approximation in wide ranges of temperature and electronic coupling strength.

Despite the good agreement with the BJ formula in the case of weak electronic coupling, one might ask how accurate the present approach is for the evaluation of the ET rate in the intermediate to strong electronic coupling regime. Since the exact quantum mechanical calculations are not trivial for multidimensional systems, we have used the one-dimensional quantum mechanical flux−flux correlation function approach to test our semiclassical formula. Since the effective one-dimensional mapping works well in the present model, we can easily compute the corresponding ET rate accurately.[54,60]

In Figure 6, we show the ET rates from the quantum mechanical flux−flux correlation approach in comparison with the present ones. It shows that the present semiclassical results are in very good agreement with the quantum in the wide range of coupling strength tested. To investigate the adiabatic limit, we also calculate the rate from the flux−flux correlation function with use only of the lower adiabatic potential energy curve, that is, we ignore the contribution from the upper adiabatic potential curve. The results are shown by the dotted line in Figure 6. One finds the present semiclassical result indeed tends to the adiabatic limit when $H_{AB} > 0.013$.

In Figure 6, the rate increases with the increase of coupling strength toward the adiabatic limit. It should be noted that this is different from the case of the solvent-controlled adiabatic limit where the rate saturates at the strong coupling limit and the saturation value is determined by the dielectric relaxation time.

Although the present formulation is general and should work equally well in the asymmetric systems, it would be better to be able demonstrate that idea. In the following subsection, we investigate this case.

5.3. Electron Transfer in the Case of Asymmetric Reaction. We use a similar potential system as in the symmetric case in the previous subsections except that the endothermicity is taken to be $3\omega_2$. With this parameter, the ET transfer still occurs in the Marcus normal region, but the potential crossing

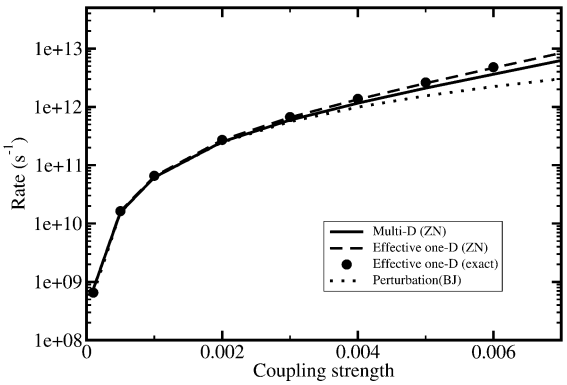

Figure 7. ET rate vs the electronic coupling strength H_{AB} at $T = 500$ K for the asymmetric reaction ($\Delta G = -3\omega_2, \omega_2 = 749$ cm^{-1}). The solid line represents the present full-dimensional result with use of the ZN formula; the dotted line represents the full-dimensional result obtained from the Bixon−Jortner formula. The filled dots represent the effective one-dimensional result of the quantum mechanical flux−flux correlation function. The dashed line represents the effective one-dimensional result with use of the ZN formula.

point in the effective one-dimensional model is shifted to the reactant side about 2/3 compared with the symmetric case. With the use of the similar procedure in the previous subsections, we have calculated the rate constants as a function of electronic coupling strength H_{AB} and the results are shown in Figure 7. In the simulation, we have found that the reaction becomes delocalized in the full-dimensional system when the coupling strength is larger than 0.007 au.

Some interesting features can be observed in Figure 7. First, the rates obtained from the ZN (solid line) and BJ (dotted line) formulas give the same rates in the small coupling regime, as it should be. However, when the coupling becomes large, the BJ formula breaks down as in the symmetric reaction. Thus, we may say that the perturbation theory does not necessarily predict the larger rate than the real one in the strong electronic coupling regime. A second interesting feature is that the rates obtained both from the ZN formula and from the flux−flux correlation function in the effective one-dimensional model agree well as in the symmetric reaction, which confirms the accuracy of the ZN formula in the general asymmetric case. Finally, we notice that the rates obtained from the effective one-dimensional model agree quite well with those from the full-dimensional calculation in the weak-to-intermediate coupling regime. In the strong electronic coupling regime, however, the one-dimensional model does not work so well as in the symmetric case.

6. Concluding Remarks

On the basis of the generalized nonadiabatic transition-state theory of thermal rate constant, we have proposed a semiclassical approach to evaluate the ET rate constant. Under the assumption of fast solvent relaxation, a new simple yet accurate formula has been derived in the Marcus' normal regime with use of the ZN (Zhu−Nakamura) theory of nonadiabatic transition. The formula is comprised of two factors: the Marcus' high-temperature formula and a prefactor to that formula. The latter contains the thermally averaged ZN transition probability and takes care of the nonadiabatic effects properly including the nuclear tunneling. Thus, the formula is a kind of extension of the Marcus−Hush formula and can cover the whole range of electronic coupling strength from the nonadiabatic to adiabatic limit. Numerical tests not only confirmed the accuracy but also demonstrated the applicability to multidimensional systems. It has also been found that the formula in the effective one-dimensional model nicely works for symmetric reactions, if we use the effective frequency proposed by Dogonadze.[25] Its validity is, however, somewhat doubtful in the asymmetric reactions in the strong coupling regime. Although the present work has discussed the statistical part of the rate constant by using a model of several intramolecular modes, the fast solvent relaxation mode, if necessary, can be taken into account on the same footing as an intramolecular mode.[61] The similar studies in the Marcus inverted regime are left for future investigation. Since the present formula in the effective one-dimensional model is quite simple in the symmetric case, we can expect that this is useful to directly explain experimental data of self-exchange reactions in the case of a fast solvent relaxation.

Open questions left for future study are (i) the recrossing effect in the strong electronic coupling regime, (ii) the dynamical solvent effect, and (iii) application to more realistic systems. As for the first problem, the Redfield theory[62] and other quantum mechanical approaches[63−65] show that the dynamical recrossing becomes important and even the vibrational coherence appears in the weak system−bath damping limit. In this case, we can employ the surface hopping technique and the idea of Wolynes[66,67] to obtain a transmission coefficient. How to incorporate the second effect, that is, the solvent dynamical effect for an arbitrary solvent, is an open question in the present approach. However, in the limit of strong damping of solvent mode, the motion of the solvent coordinate approximately satisfies the Smoluchowski equation while intramolecular and fast solvent modes determine the "sink" under the assumption of the thermal equilibrium distribution.[2,47,68,69] In this sense, the present result of eq 10 may be directly used as the sink function for the fast modes. As for the last problem, the present approach should be applicable to such systems eventually, since the ZN formula can predict the transition probabilities quite well for general curve crossing problems, although we have to overcome some problems such as the availability of accurate potentials and couplings, and also of good experiments with which to be directly compared.

Acknowledgment. We would like to thank Dr. Tachiya of AIST (National Institute of Advanced Industrial Science and Technology) for simulating discussions and critical reading of the manuscript. Y.Z. thanks Prof. Nelsen for his offer of the resonance Raman spectroscopy parameters used in the present simulation. This work was supported by the National Science Foundation of China (20333020,20473080), the 973 project funded by the National Basic Research Program of China (No. 2004CB719901) and by the Grant-in-Aid for Specially Promoted Research on "Studies of Nonadiabatic Chemical Dynamics based on the Zhu−Nakamura theory" from MEXT, Japan.

Appendix A. Thermally Averaged Transition Probability Based on the Zhu−Nakamura Formulas

In this appendix, we explicitly present the ZN formulas used for the evaluation of thermally averaged transition probability (eq 3)

$$P_T(\beta,\mathbf{Q}) = \beta \int_0^\infty \mathrm{d}E\, \mathrm{e}^{-\beta(E-V_1(\mathbf{Q}))} P_{ZN}(E,\mathbf{Q}) \qquad \text{(A-1)}$$

where $V_1(\mathbf{Q})$ is the diabatic potential and $P_{ZN}(E,\mathbf{Q})$ is the nonadiabatic transition probability. Once the nuclear coordinate $\mathbf{Q}$ is specified on the crossing seam surface, we take the direction normal to the seam across $\mathbf{Q}$ by

$$\mathbf{n} = \nabla S(\mathbf{Q})/|\nabla S(\mathbf{Q})| \qquad \text{(A-2)}$$

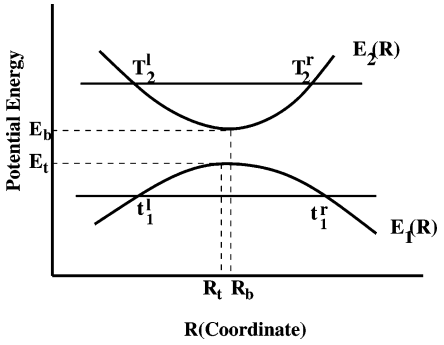

Figure 8. Schematic two-state adiabatic potentials in the case of nonadiabatic tunneling.

and cut the potential energy surfaces along this direction to obtain one-dimensional potential curves. Since the Marcus' normal case is considered in the present model, the potential curves correspond to the nonadiabatic tunneling case as shown in Figure 8. In this case, Zhu and Nakamura have provided the analytical expressions of nonadiabatic transition probability and the overall transmission probability from the left to the right along the lower adiabatic potential curve. These expressions are separately given for three energy regions ($E > E_b$, $E_b > E > E_t$, $E < E_t$) in terms of the following two parameters

$$a^2 = \sqrt{d^2 - 1}\,\frac{\hbar^2}{(T_2^{\,0} - T_1^{\,0})^2[E_2(R_0) - E_1(R_0)]} \quad \text{(A-3)}$$

and

$$b^2 = \sqrt{d^2 - 1}\,\frac{E - [E_2(R_0) + E_1(R_0)]/2}{[E_2(R_0) - E_1(R_0)]^2} \quad \text{(A-4)}$$

where

$$d^2 = \frac{[E_2(T_1^{\,0}) - E_2(T_1^{\,0})][E_1(T_2^{\,0}) - E_1(T_2^{\,0})]}{[E_2(R_0) - E_1(R_0)]^2} \quad \text{(A-5)}$$

(1) $E > E_b$: The overall transmission probability is given by

$$P_{ZN}(E) = \frac{4\cos^2\psi}{4\cos^2\psi + p^2/(1-p)} \quad \text{(A-6)}$$

where p is the probability for one passage of the crossing and takes the form

$$p = \exp\left[-\frac{\pi}{4a}\left(\frac{2}{b^2 + \sqrt{b^4 - 0.72 + 0\text{l}62a^{1.43}}}\right)^{1/2}\right] \quad \text{(A-7)}$$

and ψ is the phase factor coming from the upper adiabatic potential curve.[50−52] If one averages the phase factor, then eq A-6 becomes the conventional transmission probability with the LZ probability replaced by eq A-7.

(2) $E_b \geq E \geq E_t$: In this case, the energy locates between the top of the lower adiabatic potential and the bottom of the upper adiabatic potential. The transmission probability takes the form

$$P_{ZN}(E) = \frac{W^2}{1 + W^2} \quad \text{(A-8)}$$

where W is given by

$$W = \frac{1 + g5}{a^{2/3}}\int_0^\infty \mathrm{d}t \cos[t^3/3 - b^2 t/a^{2/3} - g_4 t/ (0.61a^{2/3}\sqrt{2 + b^2} + at)] \quad \text{(A-9)}$$

(3) $E < E_t$: In this energy region, the total transmission probability is expressed as

$$P_{ZN}(E) = \frac{B(\sigma_c/\pi)e^{-2\delta}}{[1 + (0.5\sqrt{a^2}/(1 + \sqrt{a^2}))B(\sigma_c/\pi)e^{-2\delta}]^2 + B(\sigma_c/\pi)e^{-2\delta}} \quad \text{(A-10)}$$

where nuclear tunneling is incorporated via the Gamov factor $e^{-2\delta}$, $B(x) = 2\pi x^{2X}e^{-2x}/(x\Gamma(x))$, and σ_c is the phase due to the nonadiabatic transition (see refs 50, 51, and 52). The probability of eq A-10 is always smaller than the penetration probability through the lower adiabatic potential because of the nonadiabatic coupling effect. When the diabatic coupling is infinitely strong, that is, a^2 approaches to zero, eq A-10 naturally goes to the ordinary tunneling probability $P_{ZN}(E) = e^{-2\delta}/(1 + e^{-2\delta})$.

Appendix B. Effective Mapping Frequency and One-Dimensional Potentials

One way to define the one-dimensional mapping frequency is to take the one-dimensional mode along the hopping direction, that is, the direction normal to the seam surface at MECP. With normal-mode analysis at MECP of the potentials given by eqs 26 and 27, we can obtain two shifted one-dimensional potential energy curves as

$$V_1(Q) = \frac{1}{2}\omega^2 Q_n^{\,2} + \omega'^2 Q_n + E_{TS} \quad \text{(B-1)}$$

and

$$V_2(Q) = \frac{1}{2}\omega^2 Q_n^{\,2} - \omega'^2 Q_n + E_{TS} \quad \text{(B-2)}$$

where

$$\omega^2 = \sum_i \omega_i^{\,4}\lambda_i / \sum_i \omega_i^{\,2}\lambda_i \quad \text{(B-3)}$$

$$\omega^{2'} = \frac{1}{2}\sqrt{\sum_i \omega_i^{\,2}\lambda_i} \quad \text{(B-4)}$$

and

$$E_{TS} = \frac{1}{4}\lambda + \Delta G \quad \text{(B-5)}$$

In eqs B-3 and B-5, λ_i and λ are the reorganization energy for the ith mode and the total reorganization energy, respectively. The second way is to take the effective frequency as

$$\omega^2 = \frac{1}{\lambda}\sum_i \omega_i^{\,2}\lambda_i \quad \text{(B-6)}$$

This is the method proposed by Dogonadze.[25] The corresponding potential energy curves are

$$V_1(Q) = \frac{1}{2}\omega^2 Q^2$$

and

$$V_2(Q) = \frac{1}{2}\omega^2(Q - Q_0)^2 + \Delta G \qquad \text{(B-7)}$$

with

$$Q_0 = \frac{1}{\omega}\sqrt{2\lambda} \qquad \text{(B-8)}$$

From the numerical test, we have found that the rate with use of the effective frequency given by eq B-6 gives an excellent agreement with the multi-mode simulation in the whole range of electronic coupling strength under the model of harmonic potentials and the Condon approximation.

References and Notes

(1) Zhao, Y.; Mil'nikov, G.; Nakamura, H. *J. Chem. Phys.* **2004**, *121*, 8854.
(2) Zusman, L. D. *Chem. Phys.* **1980**, *49*, 295.
(3) Burshtein, A. I. *Chem. Phys.* **1979**, *40*, 289.
(4) Barzykin, A. V.; Frantsuzov, P. A.; Seki, K.; Tachiya, M. *Adv. Chem. Phys.* **2002**, *123*, 511.
(5) Calef, D. F.; Wolynes, P. G. *J. Phys. Chem.* **1983**, *87*, 3387.
(6) Hynes, J. T. *J. Chem. Phys.* **1986**, *90*, 3701.
(7) Rips, I.; Jortner, J. *J. Chem. Phys.* **1988**, *88*, 818.
(8) Marcus, R. A. *J. Chem. Phys.* **1956**, *24*, 966.
(9) Marcus, R. A.; Sutin, N. *Biochim. Biophys. Acta* **1985**, *811*, 265.
(10) Levich, V. G.; Dogonadze, R. R. *Proc. Acad. Sci. USSR (Phys. Chem.)* **1959**, *124*, 9.
(11) Levich, V. G. *Adv. Electrochem. Electrochem. Eng.* **1965**, *4*, 249.
(12) Ao, P.; Rammer, J. *Phys. Rev. Lett* **1989**, *62*, 3004.
(13) Kim, H. J.; Hynes, J. T. *J. Chem. Phys.* **1990**, *93*, 5211.
(14) Marcus, R. A. *J. Phys. Chem.* **1992**, *96*, 1753.
(15) Gehlen, J. N.; Chandler, D.; Kim, H. J.; Hynes, J. T. *J. Phys. Chem.* **1992**, *96*, 1748.
(16) Gehlen, J. N.; Chandler, D. *J. Chem. Phys.* **1992**, *97*, 4958.
(17) Song, X.; Stuchebrukhov, A. A. *J. Chem. Phys.* **1993**, *99*, 969.
(18) Stuchebrukhov, A. A.; Song, X. *J. Chem. Phys.* **1994**, *101*, 9354.
(19) Kayanuma, Y.; Nakayama, H. *Phys. Rev. B* **1998**, *57*, 13099.
(20) Georgievskii, Y.; Stuchebrukhov, A. A. *J. Chem. Phys.* **2000**, *113*, 10438.
(21) Hush, N. S. *Coord. Chem. Rev.* **1985**, *64*, 135.
(22) Landau, L. D. *Phys. Z. Sowjetunion* **1932**, *2*, 46.
(23) Zener, C. *Proc. R. Soc. London, Ser. A* **1932**, *137*, 696.
(24) Stueckelberg, E. C. G. *Helv. Phys. Acta* **1932**, *5*, 369.
(25) Dogonadze, R. R.; Urushadze, Z. D. *J. Electroanal. Chem.* **1971**, *32*, 235.
(26) Kuki, A. *J. Phys. Chem.* **1993**, *97*, 13107.
(27) Rips, I.; Pollak, E. *J. Chem. Phys.* **1995**, *103*, 7912.
(28) Rips, I. *J. Chem. Phys.* **2004**, *121*, 5356.
(29) Tully, J. C.; Preston, R. K. *J. Chem. Phys.* **1971**, *55*, 562.
(30) Webster, F.; Rossky, P. J.; Friesner, R. A. *Comput. Phys. Commun.* **1991**, *63*, 494.
(31) Coker, D. F.; Xiao, L. *J. Chem. Phys.* **1995**, *102*, 496.
(32) Zhu, C.; Nobusada, K.; Nakamura, H. *J. Chem. Phys.* **2001**, *115*, 11036.
(33) Zhu, C.; Kamisaka, H.; Nakamura, H. *J. Chem. Phys.* **2002**, *116*, 3234.
(34) Zahr, G. E.; Preston, R. K.; Miller, W. H. *J. Chem. Phys.* **1975**, *62*, 1127.
(35) Heller, E. J.; Brown, R. C. *J. Chem. Phys.* **1983**, *79*, 3336.
(36) Lorquet, J. C.; Leyh-Nihant, B. *J. Phys. Chem.* **1988**, *92*, 4778.
(37) Remacle, F.; Dehareng, D.; Lorquet, J. C. *J. Phys. Chem.* **1988**, *92*, 4784.
(38) Marks, A. J.; Thompson, D. L. *J. Chem. Phys.* **1992**, *96*, 1911.
(39) Marks, A. J. *J. Chem. Phys.* **2001**, *114*, 1700.
(40) Topaler, M. S.; Truhlar, D. G. *J. Chem. Phys.* **1997**, *107*, 392.
(41) Cui, Q.; Morokuma, K.; Bowman, J. M. *J. Chem. Phys.* **1999**, *110*, 9469.
(42) Miller, W. H. *Chem. Rev.* **1987**, *87*, 19.
(43) Nelsen, S. F.; Ismagilov, R. F.; D. A. T., II. *Science* **1997**, *278*, 846.
(44) Demadis, K. D.; Hartshorn, C. M.; Meyer, T. J. *Chem. Rev.* **2001**, *101*, 2655.
(45) Ovchinnikova, M. Y. *Theor. Exp. Chem.* **1982**, *17*, 507.
(46) Sumi, H.; Marcus, R. A. *J. Chem. Phys.* **1986**, *84*, 4272.
(47) Walker, G. C.; Akesson, E.; Johnson, A. E.; Levinger, N. E.; Barbara, P. F. *J. Phys. Chem.* **1992**, *96*, 3728.
(48) Zhu, C.; Nakamura, H. *J. Chem. Phys.* **1994**, *101*, 10630.
(49) Zhu, C.; Nakamura, H. *J. Chem. Phys.* **1995**, *102*, 7448.
(50) Zhu, C.; Nakamura, H. *Adv. Chem. Phys.* **2001**, *117*, 127.
(51) Nakamura, H. *Nonadiabatic Transition: Concepts, Basic Theories and Applications*; World Scientific Pub. Co. Inc.: River Edge, NJ, 2002.
(52) Nakamura, H. *J. Theor. Comput. Chem.* **2005**, *4*, 127.
(53) Bixon, M.; Jortner, J. *J. Phys. Chem.* **1991**, *95*, 1941.
(54) Miller, W. H.; Schwartz, S. D.; Tromp, J. W. *J. Chem. Phys.* **1983**, *79*, 4889.
(55) Fenkel, D.; Smit, B. *Understanding Molecular Simulation*; Computational Science Series; Academy Press: San Diego, CA, 2002; Vol. 1.
(56) Yamamoto, T.; Miller, W. H. *J. Chem. Phys.* **2004**, *120*, 3086.
(57) Zhao, Y.; Yamamoto, T.; Miller, W. H. *J. Chem. Phys.* **2004**, *120*, 3100.
(58) Wang, F.; Landau, D. P. *Phys. Rev. Lett.* **2001**, *86*, 2050.
(59) Bixon, M.; Jortner, J. *Adv. Chem. Phys.* **1999**, *106*, 35.
(60) Zhao, Y.; Mil'nikov, G. *Chem. Phys. Lett.* **2005**, *413*, 362.
(61) Newton, M. D.; Sutin, N. *Annu. Rev. Phys. Chem.* **1984**, *35*, 437.
(62) Jean, J. M.; Friesner, R. A.; Fleming, G. R. *J. Chem. Phys.* **1992**, *96*, 5827.
(63) Topaler, M.; Makri, N. *J. Phys. Chem.* **1996**, *100*, 4430.
(64) Evans, D. G.; Nitzan, A.; Ratner, M. A. *J. Chem. Phys.* **1998**, *108*, 6387.
(65) Wynne, K.; Hochstrasser, R. M. *Adv. Chem. Phys.* **1999**, *107*, 263.
(66) Onuchic, J. N.; Wolynes, P. G. *J. Phys. Chem.* **1988**, *92*, 6495.
(67) Zhao, Y.; Li, X.; Zhen, Z. L.; Liang, W. Z. *J. Chem. Phys.* **2006**, *124*, 6495.
(68) Sumi, H.; Marcus, R. A. *J. Chem. Phys.* **1986**, *84*, 4894.
(69) Jortner, J.; Bixon, M. *J. Chem. Phys.* **1988**, *88*, 167.

ADDITIONS AND CORRECTIONS

2006, Volume 110A

Yi Zhao,* Wanzhen Liang, and Hiroki Nakamura: Semiclassical Treatment of Thermally Activated Electron Transfer in the Intermediate to Strong Electronic Coupling Regime under the Fast Dielectric Relaxation

Page 8209. Figure 6 shown is not correct. The correct figure is given here.

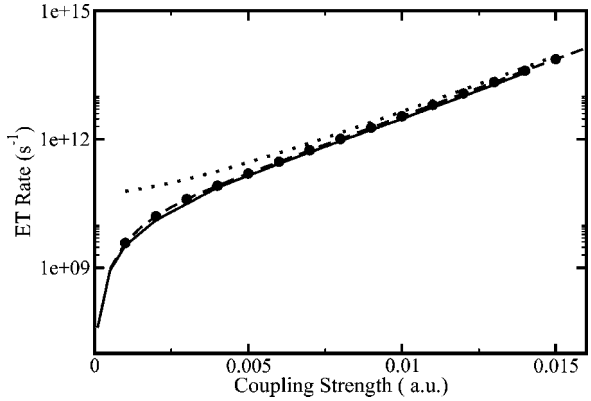

Figure 6. ET rate vs the electronic coupling strength H_{AB} at $T = 500$ K. The solid line shows the present full-dimensional result; the dashed line shows the present result in the effective one-dimensional model; the filled circle shows the result of the quantum mechanical flux−flux correlation function; the dotted line shows quantum mechanical result in the adiabatic approximation. In the case of effective one-dimensional model, the effective frequency is taken as $\omega_2 = 749$ cm^{-1}.

10.1021/jp810914v
Published on Web 12/31/2008